

Measurement of the dispersion of air and of refractive index anomalies by wavelength-dependent nonlinear interferometry

Roberto Macovez,¹ Marina Mariano,¹ Sergio Di Finizio,¹ and Jordi Martorell^{1,2}

¹ICFO-Institut de Ciències Fotoniques, 08860 Castelldefels (Barcelona), Spain

²Departament de Física i Enginyeria Nuclear, Universitat Politècnica de Catalunya, 08222 Terrassa, Spain

Abstract: We carry out wavelength-dependent second harmonic interference experiments using thin films of an organic dye as nonlinear optical sources. While the measured difference of refractive index between the fundamental and second harmonic wavelengths follows the theoretical expectation for air in a wide spectral region, anomalous dispersion is observed when the second harmonic light lies in the absorption band of the dye. The sensitivity of the technique to small refractive index variations may prove useful for sensing applications as well as for testing models of light dispersion in weakly dispersing and absorbing media.

OCIS codes: (190.2620) Harmonic generation and mixing; (120.3180) Interferometry; (300.6420) Spectroscopy, nonlinear.

References and links

1. J. Lawall, "Interferometry for Accurate Displacement Metrology," *Optics and Photonics News* **15**, 40-45 (2004).
2. K. Minoshima and H. Matsumoto, "High-accuracy measurement of 240-m distance in an optical tunnel by use of a compact femtosecond laser," *Appl. Opt.* **39**, 5512-5517 (2000).
3. A. I. Weiss, M. Hennes, and M. W. Rotach, "Derivation of refractive index and temperature gradients from optical scintillometry to correct atmospherically induced errors for highly precise geodetic measurements," *Surv. Geophys.* **22**, 589-596 (2001).
4. Y. Salvadé, R. Dändliker, A. Courteville and M. Zickar, "Air-dispersion measurement by second-harmonic heterodyne interferometry," *Opt. Lett.* **27**, 1424 (2002).
5. K. Meiners-Hagen and A. Abou-Zeid, "Refractive index determination in length measurement by two-colour interferometry," *Meas. Sci. Technol.* **19**, 084004 (2008).
6. S. Mc Murtry, J. D. Wright and D. A. Jackson, "Sensing applications of a low-coherence fibre-optic interferometer measuring the refractive index of air," *Sensors and Actuators B* **72**, 69-74 (2001).
7. B. Edlén, "The refractive index of air," *Metrologia* **2**, 71-80 (1966).
8. P. E. Ciddor, "Refractive index of air: new equations for the visible and near infrared," *Appl. Opt.* **35**, 1566-73 (1996).
9. F. E. Jones, "Simplified equation for calculating the refractivity of air," *Appl. Opt.* **19**, 4129-4130 (1980); F. E. Jones, "The refractivity of air," *J. Res. Natl. Bur. Stand.* **86**, 27-32 (1981).
10. J. Gubler and D. Tytler, "Differential Atmospheric Refraction and Limitations on the Relative Astrometric Accuracy of Large Telescopes," *Publications of the Astronomical Society of the Pacific* **110**, 738-746 (1998).
11. R. Muijlwijk, "Update of the Edlén Formulae for the Refractive Index of Air," *Metrologia* **25**, 189 (1988).
12. G. Bönsch and E. Potulski, "Measurement of the refractive index of air and comparison with modified Edlén's formula," *Metrologia* **35**, 133-9 (1998).
13. K. P. Birch and M. J. Downs, "An updated Edlén equation for the refractive index of air," *Metrologia* **30**, 155-62 (1993).
14. K. P. Birch and M. J. Downs, "Correction to the updated Edlén equation for the refractive index of air," *Metrologia* **31**, 315-6 (1994).
15. J. C. Owens, "Optical refractive index of air: dependence on pressure, temperature and composition," *Appl. Opt.* **6**, 51-59 (1967).
16. E. R. Peck and K. Reeder, "Dispersion of air," *J. Opt. Soc. Am.* **62**, 958-962 (1972).
17. J. Zhang, Z. H. Lu and L. J. Wang, "Precision measurement of the refractive index of carbon dioxide with a frequency comb," *Opt. Lett.* **32**, 3212 (2007).
18. G. Berkovic, Y. R. Shen, G. Marowsky, R. Steinhoff, "Interference between second-harmonic generation from a substrate and from an adsorbate layer," *J. Opt. Soc. Am. B* **6**, 205 (1989).

19. O. A. Aktsipetrov, T. V. Dolgova, A. A. Fedyanin, D. Schuhmacher, G. Marowsky, "Optical second-harmonic phase spectroscopy of the Si(111)-SiO₂ interface," *Thin Solid Films* **364**, 91-94 (2000).
 20. T. V. Dolgova, A. A. Fedyanin, O. A. Aktsipetrov, G. Marowsky, "Optical second-harmonic interferometric spectroscopy of Si(111)-SiO₂ interface in the vicinity of E₂ critical points," *Phys. Rev. B* **66**, 033305 (2002)
 21. V. G. Avramenko, T. V. Dolgova, A. A. Nikulin, A. A. Fedyanin, O. A. Aktsipetrov, A. F. Pudonin, A. G. Sutyryn, D. Yu. Prokhorov, A. A. Lomov, "Subnanometer-scale size effects in electronic spectra of Si/SiO₂ multiple quantum wells: Interferometric second-harmonic generation spectroscopy," *Phys. Rev. B* **73**, 155321 (2006).
 22. R. Stolle, G. Marowsky, E. Schwarzberg, and G. Berkovic, "Phase measurements in nonlinear optics," *Appl. Phys. B* **63**, 491-498 (1996).
 23. E. Schwarzberg, G. Berkovic, and G. Marowsky, "Nonlinear interferometry and phase measurements for surface second-harmonic generation in a dispersive geometry," *Appl. Phys. A* **59**, 631-637 (1994).
 24. M. Botey, J. Martorell, J. Trull, R. Vilaseca, "Suppression of radiation in a momentum-nonconserving nonlinear interaction," *Opt. Lett.* **25**, 1177 (2000).
 25. F. J. Green, *The Sigma-Aldrich Handbook of Stains, Dyes and Indicators*, Aldrich Chemical Co.: Milwaukee, Wisconsin (1990).
 26. S. Lovell, B. J. Marquardt, B. Kahr, "Crystal violet's shoulder," *J. Chem. Soc., Perkin Trans.* **2**, 2241-2247 (1999).
 27. T. Kikteva, D. Star, and G. W. Leach, "Optical Second Harmonic Generation Study of Malachite Green Orientation and Order at the Fused-Silica/Air Interface," *J. Phys. Chem. B* **104**, 2860-2867 (2000).
 28. Y. S. Galkin and R. A. Tatevian, "The problem of obtaining formulae for the refractive index of air for high-precision EDM," *Journal of Geodesy* **71**, 483-485 (1997).
 29. S. P. Velsko and D. Eimerl, "Precise measurements of optical dispersion using a new interferometric technique," *Appl. Opt.* **25**, 1344 (1986).
 30. P. Schellekens, G. Wilkening, F. Reinboth, M. J. Downs, K. P. Birch, and J. Spronck, "Measurements of the refractive index of air using interference refractometers," *Metrologia* **22**, 279-287 (1986).
-

1. Introduction

Precise knowledge of the dispersion of light in air is crucial for accurate length interferometry [1,2], geodetic surveying [3] and ground-based astronomical observations [4], and it can be useful to measure pollution or humidity levels [5,6]. Phenomenological formulae allowing the calculation of the wavelength-dependent refractive index of air from known parameters like pressure, temperature, humidity or CO₂ content have been derived by Edlén [7] in a review paper of 1966. Several different improved models were published since then which have focused on the impact of these parameters (see [8] and references therein). The analytical expression for the refractive index differs from study to study, yielding distinct wavelength dependences, and even when the same functional form is used the intervening constants are different [7,9-16]. Moreover, to obtain expressions which are valid for distinct chemical compositions (*e.g.*, different water vapor or CO₂ content) knowledge of the optical response of the single constituent gases is necessary. This response is in general wavelength-dependent, and recent studies of light dispersion in constituent gases of air have brought forth improved models with distinct functional dependences than older work (see *e.g.* [17]). To obtain a better knowledge of the refractive index in weakly dispersing media, accurate wavelength-dependent measurements would prove useful.

We discuss here a compact, robust and simple method for measuring the spectral dependence of the refractive index based on wavelength-dependent second harmonic interferometry. The detection of anomalous dispersion due to the propagation of light through the molecular films near an absorption resonance demonstrates the high sensitivity of the probe. While second harmonic interference spectroscopy has been mainly applied to the measurement of the (relative) phase of the second harmonic light generated at specific interfaces [18-21], we show here that it holds a great potential for the accurate determination of the refractive index in weakly dispersive media which has not been exploited so far. Compared with other interferometry tools to measure light dispersion, nonlinear interference spectroscopy has the advantage of requiring light propagation only over a single path in one direction, yielding a robust, alignment-independent measurement, and avoiding the need for a sophisticated method of detection of spatial interferometric patterns to achieve high accuracy. The detection of anomalous dispersion suggests a possible application of the technique for sensing purposes.

2. Description of second harmonic interference spectroscopy and experimental setup

Second harmonic generation is a coherent parametric nonlinear process in which phase information plays a crucial role. The coherence of the process allows implementing interferometric tools based on the relative dephasing of the fundamental and double-frequency beams. Several versions of second harmonic interferometry exist [22,23], all based on the generation of second harmonic light from two consecutive sources so that generation from the second one occurs in the presence of the second harmonic field generated by the first [24]. Under such conditions, the total second harmonic intensity after the second source depends on the relative phase of the fundamental and second harmonic field impinging onto it. If the two fields (of wavelengths λ and $\lambda/2$) reach the second source with the proper phase relationship further generation of second harmonic light will occur, while a phase mismatch will lead to back-conversion of the second harmonic into the fundamental field [22,23].

The easiest implementation of this principle is obtained when the two sources lie in a (weakly) dispersive medium like air and their mutual distance is varied. By scanning the inter-source distance d , the optical path difference between the fundamental and the second harmonic beam can be varied, thus tuning the dephasing between the two fields. Since second harmonic generation depends quadratically on the fundamental field intensity, the relevant dephasing is $\Delta k \times d$ where the wavevector mismatch is given by $\Delta k = k_{\lambda/2} - 2k_{\lambda}$. The second harmonic intensity measured after both sources shows a characteristic sinusoidal modulation as a function of their distance, whose frequency Δk is a measure of the dispersion of light in the medium embedding the two sources.

While second harmonic interferometry is usually implemented with lasers operating at fixed wavelength, second harmonic interference spectroscopy is the generalization of this concept to the case of a tunable light source. By varying the pump frequency, spectral information may be obtained both on the relative phase of the second harmonic light generated at the two sources [18-22], and, which is of interest here, on the spectral dependence of the refractive index of the medium embedding them. The experiments were performed with an optical parametric oscillator (OPO) pumped by a Q-switched Nd:YAG laser operating at 10 Hz, which provides wavelength-tunable nanosecond pulses. Thin films of a nonlinear dye (crystal violet) adsorbed on microscope glass slides were used as nonlinear optical sources. The substrates were immersed into solutions of the dye in 1-propanol during few minutes and then retrieved at a constant speed of 0.3 mm/s. One side of the microscope slide was then carefully cleaned, leaving the molecular film only on the other in order to avoid second harmonic generation interferences between the two sides of the same substrate [22].

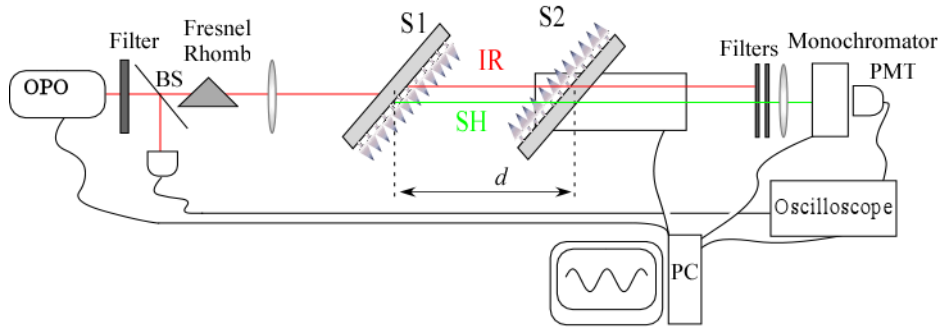


Fig. 1. Schematic diagram of the setup for second harmonic interference spectroscopy. The second source (S2) is mounted on a motorized translation stage

The setup used for the experiments is shown in Fig. 1. The idler infrared beam (IR) from the OPO, whose wavelength was tuned between 750 and 1250 nm during the experiments, was passed through a RG715 filter (Schott) to get rid of residual UV and visible radiation and

through a Fresnel rhomb to rotate its linear polarization to transverse magnetic (P-polarization) so as to maximize second harmonic generation from the thin molecular films (labeled SH in Figure 1). The reflection off a clean glass slide was used as trigger for the detection of the second harmonic signal. A lens with 100 cm focal length was employed to obtain a weakly focused beam with a relatively long Rayleigh range, which yielded a second harmonic intensity from the second source (S2 in Fig. 1) approximately constant (see Section 3). The first nonlinear source (S1) was mounted on a fixed stage while the second was placed on a motorized translation stage. In both cases the substrate normal lay at 45° with respect to the laser beam to enhance second harmonic generation. The sides covered with the dye faced one another, so that the two molecular films were only separated by air. After filtering the fundamental beam by a combination of KG5 and BG39 filters, the second harmonic light was focused into a monochromator by a lens with 10 cm focal distance, and then detected at the monochromator output with a photomultiplier tube. The interferograms were recorded by displacing the second sample over a total distance of 310 mm along the beam direction in steps of 5 mm. The position of the second sample and the data acquisition were controlled by computer using a simple LabVIEW[®] routine.

3. Results and discussion

Two examples of interferograms recorded at the second harmonic wavelengths of 470 and 550 nm, respectively, are shown in Fig. 2(a). The two films used as sources were obtained with a 8×10^{-4} M solution. The inter-source distance d is measured in millimeters, and the signal intensity is normalized between 0 and 1. All interferograms displayed only little or no drift, which demonstrates that the pump energy density remained roughly constant over the whole distance covered by the second sample. The interferograms were fitted with sine functions defined as:

$$h + a \sin(f \times d + \varphi). \quad (1)$$

It can be observed in Fig. 2(a) that the quality of the fit is rather good for both interferograms. Each of the parameters h , a , f and φ was left free to vary in the fitting procedure. The most important parameter is the frequency $f = \Delta k$ of the sinusoidal modulation, which as described in Section 2 is the wavevector mismatch in air between the square of the fundamental field and the second harmonic field. This quantity is plotted as function of the fundamental wavelength in Fig. 2(b). The relative error was lower than 0.5% for all probed wavelengths.

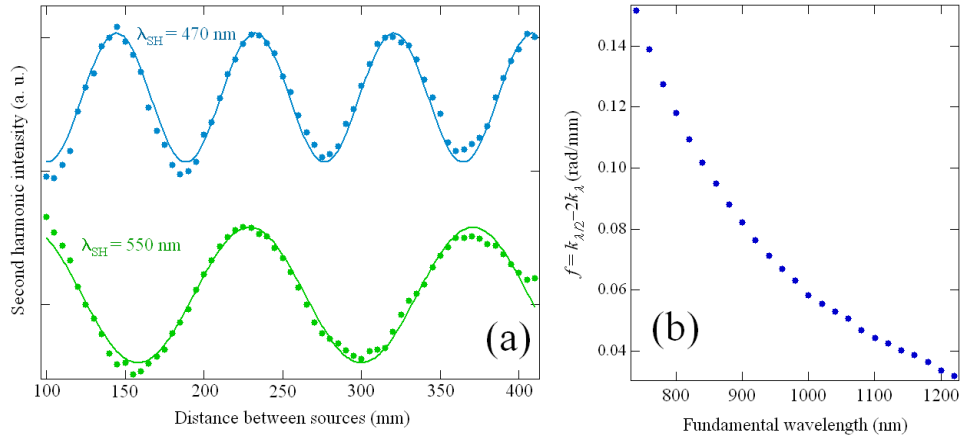


Fig. 2. (a) Second harmonic interferograms acquired at second harmonic wavelengths of 470 and 550 nm, fitted with sine functions as defined in the text. (b) Plot of the wavevector mismatch as obtained from the fitting procedure, as a function of the fundamental wavelength

Since $k_\lambda = \frac{2\pi}{\lambda}n_\lambda$, the wavevector mismatch may be written as:

$$k_{\lambda/2} - 2k_\lambda = \frac{4\pi}{\lambda}(n_{\lambda/2} - n_\lambda). \quad (2)$$

One can therefore directly extract the difference in refractive index between the wavelengths $\lambda/2$ and λ by multiplying the experimental values plotted in Fig. 1(b) by the corresponding fundamental wavelength times a constant. The result is shown in Fig. 3. Along with the experimental data we have plotted the theoretical curve corresponding to a recent phenomenological model [12] based on the modified Sellmeier equation [8]. The equation for the theoretical curve is:

$$n_{\lambda/2} - n_\lambda = \sum_i^2 B_i \left(\frac{1}{(C_i - 4/\lambda^2)} - \frac{1}{(C_i - 1/\lambda^2)} \right). \quad (3)$$

The parameters B_i and C_i are taken from Ref. 12, and correspond to the case of dry air under standard conditions as defined therein (temperature 20 °C, pressure 100 kPa, CO₂ volume fraction 0.04%).

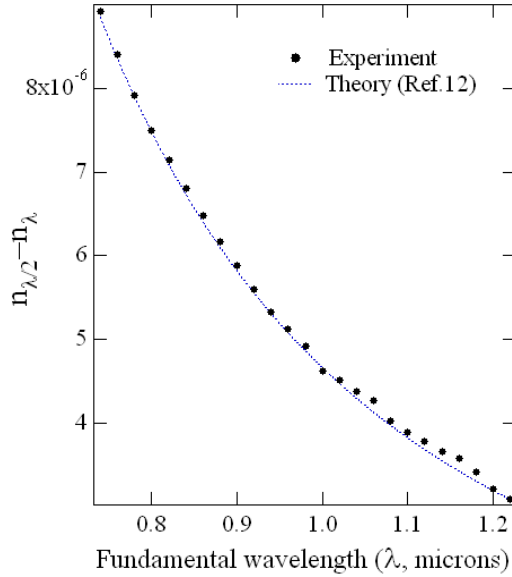


Fig. 3. Plot of the refractive index difference between λ and $\lambda/2$ in air (dots), as a function of λ . The dashed curve corresponds to the phenomenological model of Ref. 12

It can be seen in Fig. 3 that the model is in very good agreement with the experimental data apart from a range of fundamental wavelengths between 1020 and 1180 nm. In this region, the experimental dispersion appears to be less smooth than at lower wavelengths (see also Fig. 2(b)). The origin of the discrepancy for fundamental wavelengths between 1 and 1.2 microns is that the corresponding second harmonic light (between 500 and 600 nm) lies in the spectral region of absorption of the molecular dye used in the experiment [25]. We show in Fig. 4 the dispersion curve measured with thicker crystal violet films as sources, which were obtained using a more concentrated 10^{-2} M solution. The theoretical curve for air [12] is shown again for comparison. It is apparent from Fig. 4 that the measured dispersion displays, on top of the expected decay with increasing wavelength, a characteristic S-shaped modulation, which signals the presence of a molecular absorption resonance.

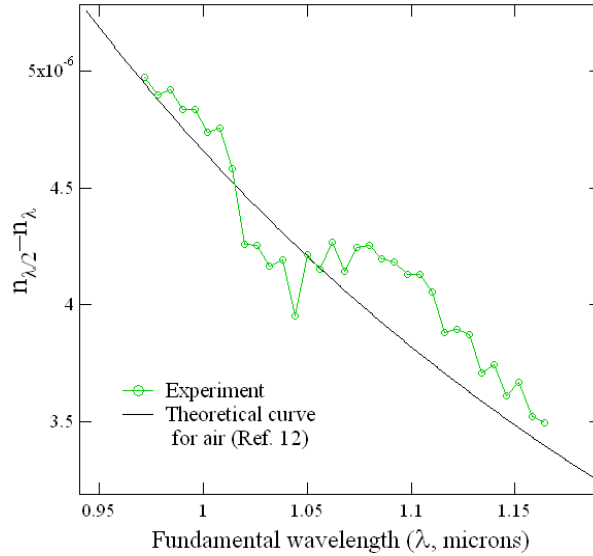


Fig. 4. Anomalous dispersion of the second harmonic light around the absorption resonance of the dye, as measured using thicker molecular films as second harmonic sources

As shown in Fig. 5, the linear extinction spectra of the adsorbed films display a broad absorption around 550 nm with two characteristic bands, which are interpreted in condensed phases as due to the formation of agglomerates and to the existence of distinct excited states [26]. While for the lower concentration the most intense absorption band is the one at longer wavelength, similar to what is reported in solution [25], for higher dye content the low-wavelength band becomes the most intense one, leading to a blueshift of the absorption maximum by approximately 40 nm. Similarly, the signature of the anomalous dispersion appears blueshifted at higher dye concentration with respect to the lower density case (Fig. 3). The extent of this blueshift is consistent with a value of twice the displacement of the absorption maximum. Hence the shape, wavelength range, and dependence upon dye coverage of the observed dispersion features unambiguously identify their origin in the molecular resonance, indicating that the dispersion anomaly is related to the propagation of light through the absorbing sources.

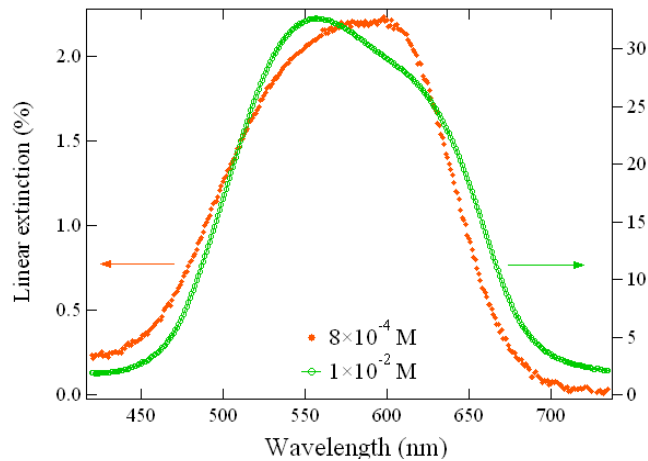


Fig. 5. Linear extinction spectra of the molecular films used as sources, for both concentrations

It is not straightforward to see why the anomalous dispersion shows up in the interferograms. In order to investigate the origin of the dispersion anomaly, we have performed second harmonic interferometry experiments as a function of the pump power, using as fundamental beam the output of the Q-switched Nd:Yag at 1064 nm. Although the laser intensity was varied by almost two orders of magnitude in these experiments, no change was detected in the period of the sinusoidal modulation. This indicates that the observation of the anomaly is most likely due to a linear effect, rather than a nonlinear one, and that it therefore involves the propagation of the visible second harmonic light through the thin films near their (linear) absorption resonance. In principle, the coefficient which multiplies the inter-source distance d in Eq. (1) should contain only the wavevector mismatch in air, since varying this distance only varies the optical path through the gas. However, eq. (1) strictly holds for a collimated pump beam without any field gradients, while the case of a focused beam is more complex. In our experiments, the second source is initially close to the focal point of the laser and moves away from it as the interferogram is recorded. This can be inferred also from Fig. 1(a), where the small decrease in amplitude observable in the interferograms is indicative of the fact that the second harmonic intensity from the second source decays as it is moved away from the focal point. Both the fundamental laser beam and the second harmonic beam generated at the first source diverge away from the focal point, so that the average angle with which the beams impinge onto the surface of the second source increases as the latter is moved away from the focus.

We argue that the observation of the anomaly in the interferograms may be related to the details of the experimental geometry. A possible explanation is that the effective optical path through the film depends on the position of the second source. This is not unlikely as the beam divergence implies that the average angle of impact θ of light rays unto the film surface grows larger as the latter is moved away from the focal point, or equivalently as the inter-source distance d is varied. Hence the average optical path $n\delta \times \left\langle \frac{1}{\cos(\theta)} \right\rangle$ through the

absorbing film increases with d (δ being the film thickness measured normal to the film surface). Such dependence contributes to modify the shape of the measured interferogram, and, although it is not a simple linear dependence, it may affect the effective periodicity of the pattern thus possibly resulting in the observation of anomalous dispersion. However, we cannot rule out that other mechanisms (perhaps also involving the nonlinear optical response) may be responsible for the observation of anomalous dispersion in the interferograms.

Since the signature of anomalous dispersion is already visible for the thinner molecular films (Fig. 3), which have a thickness of few molecular layers, we find that a very small amount of molecules of the order of a monolayer is already sufficient to give a detectable deviation from the expected dispersion in the gas. This suggests that second harmonic interferometry might be applicable to sensing small amounts of resonant (molecular or atomic) species in a gas by detecting the deviation in refractive index associated with dispersion anomalies. Since the number of molecules lying inside the beam's cross section A is $N = \sigma A$, where σ is the molecular surface density, and the interferometer volume is $V = \ell A$ with ℓ the average distance between the two sources, the same amount of molecules

would result in a volume number density $\frac{N}{V} = \frac{\sigma}{\ell}$ if they were spread in the whole volume of

the interferometer instead of on the surface of the microscope slide. Taking σ to be of the order of 10^{14} molecules per square millimeter (a typical value for a dense molecular layer on a flat surface [27]) and an interferometer length of one meter, the equivalent volume density turns out to be of the order of 10^{17} molecules per liter, that is, of the order of 10 parts per million (ppm) in air at standard conditions. The method may therefore be useful to detect the presence of resonant species in a gas with concentrations of few ppm (and possibly lower, depending on the detection accuracy).

Compared with other techniques for measuring light dispersion, second harmonic interference spectroscopy has the obvious advantage of using a tunable light source which allows obtaining measuring dispersion curves of gases (and in principle also liquids) over a wide spectral region. We point out that the same experiments can be carried out with a bulk nonlinear crystal rather than with thin-film samples, thus yielding higher conversion efficiency and a more easily detectable second harmonic signal. The use of non-resonant sources or of a collimated beam eliminates dispersion effects due to the sources, so that the intrinsic dispersion curve of the medium embedding them is obtained. By suitable fitting procedures, accurate values of the phenomenological constants entering dispersion models can then be retrieved. For example in the case of moist air, pressure or temperature variations lead to a wavelength-dependent renormalization of the dispersion, so that a simultaneous study as a function of *e.g.* pressure and wavelength yields complete knowledge of the refractive index (including the constant term in the Sellmeier expansion or similar [8]). The acquisition of data at many different wavelengths may also enable more sophisticated wavelength-dependent fits based on models which take into account broad rather than localized resonances [28]. The typical accuracy obtained in our fits implies that a precision of 10^{-9} or lower on the refractive index mismatch is easily obtained, in agreement with an earlier estimate [29]. The achievable accuracy is thus at least as good if not better than that of state-of-the-art refractometry [8,30].

4. Conclusions

In summary, we have employed second harmonic interference spectroscopy to measure the difference in refractive index between the fundamental and second harmonic frequencies in air at room temperature, and have observed the signature of anomalous dispersion in correspondence with the absorption band of the thin molecular films used as nonlinear sources. We have discussed the advantages of wavelength-dependent nonlinear interferometry over existing measurements of light dispersion, which are namely the possibility of exploring a wide continuous range of wavelengths, the propagation of light only along a single optical path in one direction, the ease of implementation, and the high sensitivity. Our results and the accuracy of the probe suggest that the method may be applied for testing gas dispersion models as well as for sensing small concentrations of molecular or atomic species in gas form based on the detection of dispersion anomalies near absorption resonances.

Acknowledgments

This work has been supported by the Spanish Ministerio de Ciencia e Innovación, under grants MAT2008-00910/NAN and CONSOLIDER NANOLIGHT CSD2007-00046. R. M. acknowledges financial support from a Juan de la Cierva fellowship granted by the same Ministry.